Available online at www.sciencedirect.com

ScienceDirect

IFAC Papers Online CONFERENCE PAPER ARCHIVE

IFAC PapersOnLine 55-27 (2022) 410–415

Preview Dynamic Chassis Control Based on Road Condition Recognition Employed Machine Vision

Libo Mao, Guangqiang Wu* , Huize Hu, Dong Zhang

School of Automotive Studies, Tongji University

CHN (Guangqiang Wu, e-mail: wuguangqiang@tongji.edu.cn).

Abstract: In order to solve the problem that the dynamic chassis control needs to passively respond after the tire touches the target object, this paper proposes a dynamic chassis control method based on fuzzy logic and road condition recognition employed machine vision. The fuzzy logic control strategy is first conducted to suppress vertical and pitch motion. Then, the camera fixed on the car window is used to take pictures of bumps or potholes and form a training data set. Based on the powerful pattern recognition capabilities of the neural network, the MATLAB neural network toolbox is used to build the convolutional neural network for data training and form the recognition operator and transfer the recognition results to the dynamic chassis controller in the form of CAN signals to make it act in advance. Based on the vibration dose value of the vertical acceleration comparison with the one without preview control of the vehicle passing the same bump or potholes, the method reduces the vertical acceleration at different vehicle speeds to corresponding degrees, which proves that the method is effective for improving the ride and comfort of the vehicle in such conditions.

Keywords: Dynamic chassis, machine vision, fuzzy logic, neural network, pattern recognition.

1. INTRODUCTION

With the rapid popularization of vehicles, people are no longer satisfied with the function of vehicles as a simple means of transportation, and the requirements for vehicle comfort are increasing. The research of suspension system with good performance is getting more and more attention. Because passive suspension is only suitable for specific road, while active suspension can adapt to various roads, but as an active control, it is expensive, structural and energy consuming, so it is not suitable for suspension control of general vehicles. As a control method between above two methods, semi-active suspension has attracted more and more attention due to its better control effect and lower cost (Ren Yongsheng et al. 2006; Chen long et al. 2020).

For vehicle semi-active suspension control, many scholars have proposed different methods, mainly including model reference adaptive control (Tianjun Z et al. 2021), preview model predictive control (Shehata Gad A. 2020), improved Fuzzy logic control (Zhang Liangxiu et al. 2020), Skyhook control(Ye Guanghu et al.2015), etc., many Bench tests and vehicle tests have been carried out based on these control methods in the literature to verify the effects. Working principle and valve system behaviour of its actuator have been studied according to the theory of hydraulics and elasticity(Deng Min et al. 2018). Although the above control methods are effective, these control methods are somewhat passive control. After the tire contacts the target object and causes the suspension to produce vertical displacement, the controller controls the actuator to act. The limitation of this method is that the response of the control has a certain delay, which leads to the suspension not being well controlled in a short time before and after the actuator acts, so the ride comfort is poor. With the continuous development of machine learning, its role in the field of pattern recognition is gradually highlighted. In order to solve the problem of control delay in dynamic chassis control, given the outstanding effect of machine learning method in the field of pattern recognition, this paper proposes a preview dynamic chassis control method, which uses machine vision and deep neural network to identify the bump or pothole ahead of the road, and calculates the relative distance between the vehicle and the target. After that, the controller calculates the starting time of the actuator and the optimized control quantity according to the speed and relative distance of the vehicle and the target, so that the actuator can act in advance and optimize the damping of the shock absorber and the vehicle will have better comfort when passing the bump or pothole.

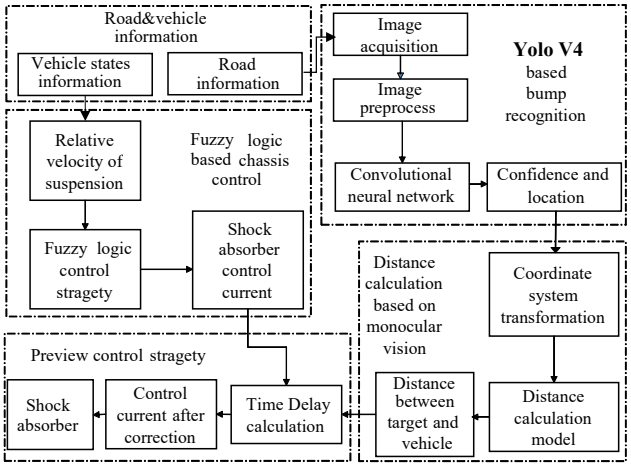

Figure 1. Framework of the study

The framework of this the method in this paper is shown in Figure 1. The rest of this paper is organized as follows. The second Section introduces the semi-active suspension quarter vehicle model and the principle and implementation of the improved ceiling control strategy. Pitch angle suppression control logic is stated in section three. In Section four, the

10.1016/j.ifacol.2022.10.565

recognition of road condition based on YOLO V4 is introduced. The calculation model of bump or pothole distance based on monocular vision is established in Section five. In the sixth Section, the preview control strategy based on the fuzzy logic control is established. The proposed preview control strategy is verified in Section seven, and the summary and future works are given in Section eight.

2. SEMI ACTIVE SUSPENSION QUARTER VEHICLE MODELING AND FUZZY CONTROL LOGIC

This paper uses fuzzy logic as the control strategy.The main function of semi-active suspension is to suppress vehicle body vibration. The signal output to the damper is the control current. Combined with the experimental analysis, the value range of these physical quantities is obtained, as shown in Table 1.

Table 1. Physical interval of observation and output

Variables	Interval	Units
Vertical acceleration	[-20,20]	m/s^2
Vertical velocity	[-0.8,0.8]	m/s
Control current	[0.29,1.6]	A

Body vertical speed and acceleration are selected as the inputs of the control system. They can be measured by onboard sensor, which is not the main work of the paper. The fuzzy set is $[NB, NS, ZO, PS, PB]$. Considering that the output of the controller is current and it is positive, the fuzzy set is $[B, PB, PM, PS, S]$.

The membership function selected by the vertical controller of suspension is triangular distribution. The domain of variables is the value range in Table 1. Figure 2-4 show the membership function of vertical fuzzy logic control of dynamic chassis.

The damping force described above needs to be converted into the control current signal. Figure 5 shows the damping characteristic curve. After the damping force is calculated, the corresponding current can be obtained through interpolation calculation combined with the relative motion speed of the shock absorber. The velocity in the Figure means the velocity of the shock absorber. The force calculated here is called U_z. The total control current will be calculated in the next section. The fuzzy rules for the suppression of vertical acceleration of vehicle body are shown in Table 2.

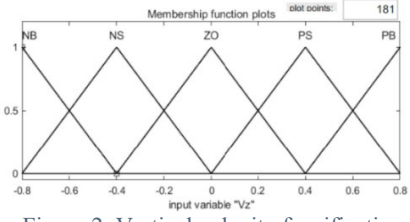

Figure 2. Vertical velocity fuzzification

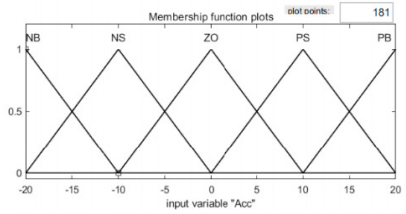

Figure 3. Vertical Acceleration fuzzification

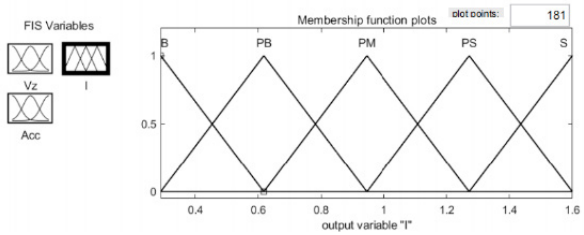

Figure 4. Output current fuzzification

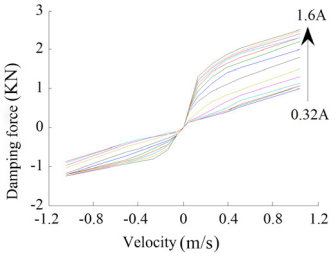

Figure 5. Damping characteristics of shock absorber

Table 2. Fuzzy rules for suppressing vertical vibration

$\dot{z}$ \ $\ddot{z}$	NB	NS	ZO	PS	PB
NB	B	PB	PM	PS	PB
NS	PB	PM	S	PS	PM
ZO	PM	PS	S	S	PM
PS	PS	PS	S	PS	PB
PB	PS	PM	PM	PB	B

3. VEHICLE PITCH CONTROL STRATEGY BASED ON FUZZY LOGIC

This paper selects the semi-active suspension 1/2 vehicle model (Zhang Liangxiu, et al. 2020; Zhang Xiangrui et al. 2018;Wu Guangqiang, et al. 2021), as shown in Figure 6.

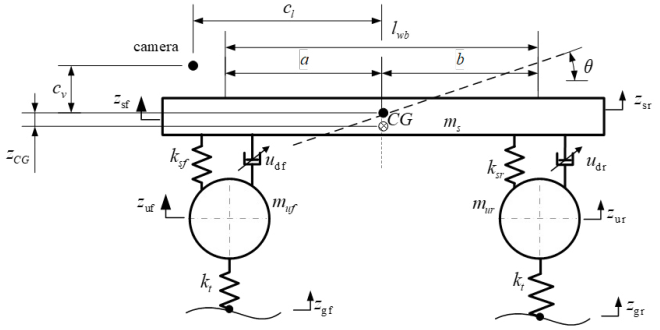

Figure 6. Semi active suspension 1 / 2 vehicle model

The dynamics equation corresponding to Figure 6 is as follows.

$$I_y\ddot{\theta} = -a\cdot u_{df} + b\cdot u_{dr} - a\cdot k_s\left(z_{sf} - z_{uf}\right) + b\cdot k_s\left(z_{sr} - z_{ur}\right) \quad (1)$$

Where, I_y is the moment of inertia about Y-axis. u_{df} 、 u_{dr} are damping force. θ is the pitch angle. l_{CG} is displacement of CG. z_{sf} 、 z_{sr} are the sprung mass. a and b are the distance from the front and rear axles to CG. z_{uf} 、 z_{ur} are the unsprung mass of the front axle and the rear axle respectively.

In order to suppress vehicle pitch, an additional pitch moment needs to be added, so equation (1) is rewritten as follows.

$$I_y\ddot{\theta} = -a\cdot u_{df} + b\cdot u_{dr} - a\cdot k_s\left(z_{sf} - z_{uf}\right) + b\cdot k_s\left(z_{sr} - z_{ur}\right) - \Delta M_y \quad (2)$$

Body pitch angle e and angular velocity $\dot{e}$ are selected as the inputs of the fuzzy logic control logic. The fuzzy rules is listed in Table 3.

Table 3. fuzzy rules for anti-pitch

$\dot{e}$ \ e	NB	NS	ZO	PS	PB
NB	PB	PB	PB	NS	NB
NS	PB	PS	ZO	NS	NB
ZO	PS	ZO	ZO	ZO	NS
PS	PS	PS	ZO	NS	NS
PB	PB	PS	PS	NB	NB

The fuzzy logic controller outputs the anti-pitch moment, which needs to be converted to the suspension damping force in combination with the distance between the center of mass and the front/rear axles. The control strategy is as follows.

a. When $\Delta M_y \cdot (\dot{z}_{sf} - \dot{z}_{uf}) > 0$, $\Delta M_y \cdot (\dot{z}_{sr} - \dot{z}_{ur}) > 0$

$$\begin{cases} \Delta F^{P}_{d,fl} = \Delta F^{P}_{d,fr} = -\Delta M_y / (2a) \\ \Delta F^{P}_{d,rl} = \Delta F^{P}_{d,rr} = 0 \end{cases} \quad (3)$$

b. When $\Delta M_y \cdot (\dot{z}_{sf} - \dot{z}_{uf}) \le 0$, $\Delta M_y \cdot (\dot{z}_{sr} - \dot{z}_{ur}) \le 0$

$$\begin{cases} \Delta F^{P}_{d,fl} = \Delta F^{P}_{d,fr} = 0 \\ \Delta F^{P}_{d,rl} = \Delta F^{P}_{d,rr} = \Delta M_y / (2b) \end{cases} \quad (4)$$

Where, $\Delta F^{P}_{d,fl}$、$\Delta F^{P}_{d,rl}$、$\Delta F^{P}_{d,fr}$ and $\Delta F^{P}_{d,rr}$ are the anti-pitch additional damping forces of the front left, rear left, front right and rear right shock absorbers respectively. $\dot{z}_{sf}$ and $\dot{z}_{uf}$ is the vertical acceleration of sprung mass and unsprung mass respectively. When the moving direction of the front and rear axle suspension is inconsistent, the vehicle will have a large roll angle and the roll angle is increasing. The control force of the four shock absorbers is as shown in formula (5), and the direction is opposite to the direction of suspension movement.

$$\Delta F^{P}_{d,fl} = \Delta F^{P}_{d,fr} = \Delta F^{P}_{d,rl} = \Delta F^{P}_{d,rr} = |\Delta M_y / 2(a+b)| \quad (5)$$

The force calculated here is named U_{Pitch}. According to section 2, the total control force of the shock absorber is as follows:

$$U = U_z + U_{Pitch} \quad (6)$$

According to Figure 6 in section 2, the control current shall be calculated via interpolation.

4. RECOGITION OF ROAD BASED ON YOLO V4

4.1 Basic Principle of YOLO Deep Convolution Neural Network

Joseph et al. first proposed a target detection method named YOLO (you only look once).

Based on the v1 version, YOLO v2 (Wei Yongming et al. 2017) and YOLO v3 (Redmon J et al. 2018) have been proposed in succession. The V4 version further improves the network structure and training methods on the basis of the v3 version (Qiao S et al. 2020).

4.2 Road Concave/Convex Recognition Based on YOLO V4

The vehicle coordinate system shall be defined as follows. The vehicle's centroid is taken as the origin of the coordinates and the forward direction of the vehicle as the X axis, the left direction as the Y axis, and the upward direction along the gravity direction as the Z axis. The installation position parameters of the camera are shown in Figure 6.

Using the image labeling plug-in tool named LabelImg in python to mark the bumps or potholes in the pictures (Lin M et al. 2019), the data sets collected in Tongji University is formed. The detection method is trained using python based on YOLO v4. Figure 7 shows an example of the recognition result.

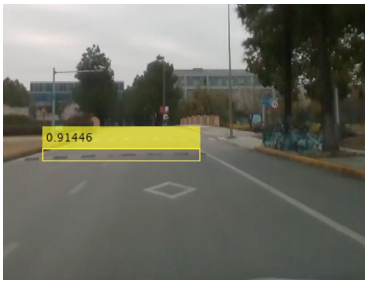

Figure 7. Example of recognition effect of bump

5. CALCULATION OF BUMP OR POTHOLE DISTANCE BASED ON MONOCULAR CAMERA

Camera based distance measurement belongs to computer vision three-dimensional measurement technology, which needs to obtain three-dimensional world information from two-dimensional images. This paper uses monocular vision based ranging method because of low cost and good convenience.

Before the distance calculation, the camera is calibrated according to Zhang Zhengyou calibration method.

The imaging principle of the camera is similar to that of the small hole imaging. This paper uses the above principle for distance calculation. It will not be expanded here for space reasons.

6. PREVIEW CONTROL STRATEGY

6.1 Communication Between Python and MATLAB Based on TCP / IP And Signal Preprocessing

This paper uses TCP / IP communication mode (Comer et al. 1993) to send messages between Python and MATLAB.
Because the recognition algorithm has a certain error recognition rate, this paper sets a target object trust threshold, only when the confidence is greater than the threshold, the recognized object is considered to be the bump or pothole. In this paper, the threshold is 0.8.

$$label = \begin{cases} 1 & 0.8 < conf \le 1 \\ 0 & 0 \le conf \le 0.8 \end{cases} \quad (7)$$

Where *label* represents the existence of the bump, *conf* represents the confidence level.

6.2 Design of Preview Control Strategy

The control current has been obtained according to the Fuzzy logic control strategy. This paper considers that this value can be used as the base current value that the controller should output.

After the target object signal is received, the current correction signal will be sent after a period of time. The delay time of the front and rear wheels should be calculated separately.

The paper uses $\overline{v}_{lon}$ to represent average longitudinal speed. Thus,the delay time,the response delay time of rear wheel to front wheel and the response time delay of the rear wheel can be calculated as follows.

$$d_{TF}=\frac{Dist}{\overline{v}_{Lon}},\quad d_{TFR}=\frac{l_{wb}}{v_{lon}},\quad d_{\mathrm{TR}}=d_{\mathrm{TF}}+d_{\mathrm{TFR}} \tag{8}$$

Where, *Dist* is the relative distance between the target and the vehicle, $\overline{v}_{lon}$ is the average vehicle longitudinal speed obtained 5s before the target is detected.

After many tests, a threshold value is taken for the suspension dynamic deflection. The coefficient is showed in Table 4.

$$I_x'=\sigma I_x \tag{9}$$

Where I_x' is the control current of the damper solenoid valve calculated by the fuzzy logic control strategy; *x* represents each damper solenoid valve.

Table 4. Current correction coefficient under different speeds

Coefficients / Speed (km/h)	Front (Bump)	Rear (Bump)	Front (Pothole)	Rear (Pothole)
$10<v\le 20$	0.90	0.92	1.11	1.09
$20<v\le 30$	0.80	0.82	1.25	1.22
$30<v\le 50$	0.90	0.92	1.11	1.09
$v\ge 50$	0.96	0.98	1.32	1.30

7. EXPERIMENTAL VERIFICATION

7.1 Simulation Verification

The control strategy based on above strategy is built in MATLAB/Simulink.

This paper establishes a stochastic road. According to the regulations of ISO2631, the power spectral density of road displacement $G_q(n)$ can be expressed using a fitting expression in the form of a power function:

$$G_q(n)=G_q(n_0)\left(n/n_0\right)^{-W} \tag{10}$$

In the formula: *n* is the spatial frequency and the unit is m^{-1}; n_0 is the reference spatial frequency, $n_0=0.1\mathrm{m}^{-1}$; $G_q(n_0)$ is the road roughness coefficient under the reference spatial frequency and the unit is $\mathrm{m}^2/\mathrm{m}^{-1}$; *W* is the frequency index.

The roughness of different grades of roads is generally reflected by the roughness coefficient G_0, and the road spectrum of a rough road can often be obtained by summing the different spectrums of a smooth road at a certain ratio.

In general, the value of G_0 is 3×10^{-8}~5×10^{-7}. Assuming that the vehicle speed is v_{x}, the following formula can be obtained:

$$\dot{z}_{\mathrm{g}}(t)=-2\pi f_0 z_{\mathrm{g}}(t)+2\pi\sqrt{G_0 v_{\mathrm{x}}}\,w_{\mathrm{g}}(t) \tag{11}$$

Where, $w_{\mathrm{g}}(t)$ is the Gaussian white noise with zero mathematical expectation, and f_0 is the spatial cut-off frequency, $f_0\approx0.01\mathrm{Hz}$.

Table 5. Vehicle simulation parameters

parameters	values	units
Gross Vehicle Weight m	1475	kg
Sprung mass m_s	1315	kg
Unsprung mass m_v	160	kg
Vehicle CG height h	0.35	m
Distance from CG to front axle a	1.050	m
Distance from CG to rear axle b	1.606	m
Longitudinal distance of camera to CG c_l	1.03	m
Vertical distance of camera to CG c_v	0.3	m
Front suspension stiffness k_{sf}	27000	N/m
Rear suspension stiffness k_{sr}	27000	N/m
Tire vertical stiffness k_{tf}	230000	N/m

Vibration dose value (VDV) is the cumulative value of whole-body vibration measurement. The calculation formula of vibration evaluation index VDV is as follows:

$$\mathrm{VDV}=\left\{\int_0^T\left[a_{\mathrm{w}}(t)\right]^4\mathrm{d}t\right\}^{\frac{1}{4}} \tag{12}$$

Where, $a_{\mathrm{w}}(t)$ is acceleration time history, m/s; T is the calculated length of time.

The vehicle is tested to pass through the road at speed 25 km/h and 35 km/h. The simulation test results are shown in Figure 8(a), (b) and Table 6.

The value of vibration dose value is reduced by 29.60%. Similarly, when the vehicle speed is 35 km/h, the VDV is reduced by 16.87%.

According to the results shown in Figure 8(a), (b), in this simulation experiment, the vibration with or without preview control strategy is in low frequency (< 2Hz).

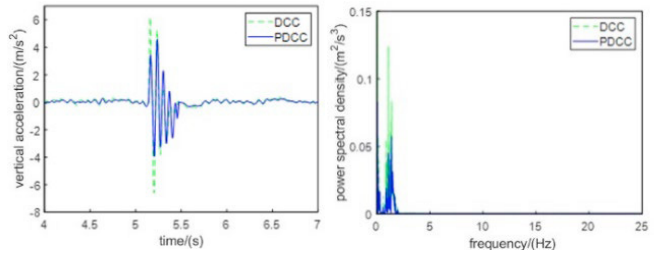

vertical acceleration power spectral density

(a) Simulation test results of passing a single bump at a constant speed (25km / h)

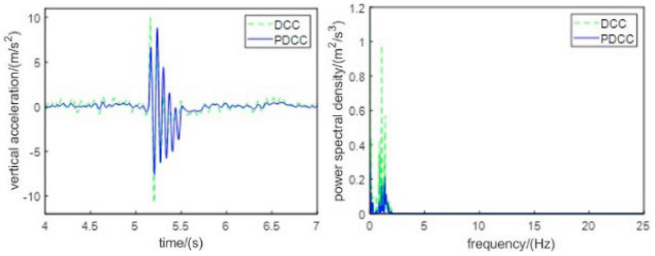

vertical acceleration power spectral density

(b) Simulation test results of passing a single bump at a constant speed (35km / h)

Figure 8. Comparison of test results at different speeds

VDV Without Preview and VDV Without Preview are labeled as V_{wo} and V_w. Improvement is stated as IMP and it is calculated as follows.

$$\mathrm{IMP} = \frac{V_{wo} - V_w}{V_{wo}} \tag{13}$$

Table 6. Simulation test results of bump and pothole

Indices/variables / condition	Speed (km/h)	VDV Without Preview (m/s1.75)	VDV With Preview (m/s1.75)	Improvement
Bump	25	3.6816	2.5920	29.60%
	35	5.9652	4.9589	16.90%
Pothole	25	3.8053	2.8290	25.66%
	35	4.9695	3.3385	32.82%

For pothole, the vehicle is tested to pass through the road at speed 25 km/h and 35 km/h. The preview control effect of this working condition is shown in Figure 9(a), (b) and Table 7.

The VDV is reduced by 25.66% and 32.82% at 25 km/h and 35 km/h respectively.

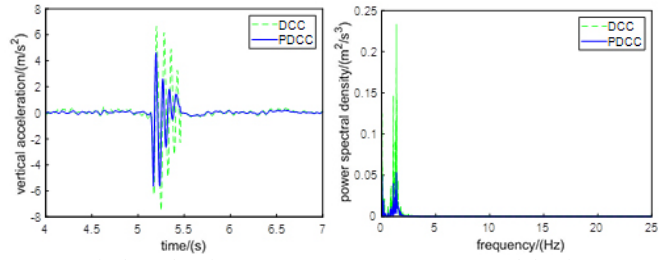

vertical acceleration power spectral density

(a) Simulation test results of passing a single bump at a constant speed (25km / h)

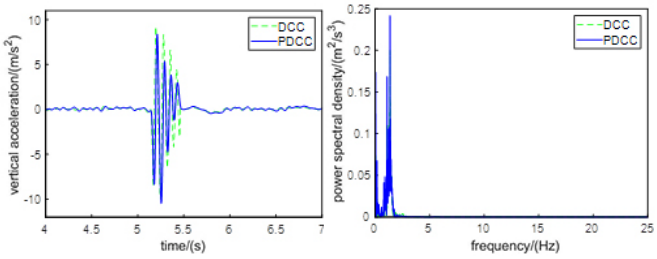

vertical acceleration power spectral density

(b) Simulation test results of passing a single bump at a constant speed (35km / h)

Figure 9. Comparison of test results at different speeds

7.2. Vehicle Verification

This paper uses a self-developed dynamic chassis controller (DCC controller) to control the shock absorber.

Through the CAN module of Simulink, the recognized bump information is sent to the DCC controller, which controls the shock absorber according to the control logic described above.

Because there are no testable potholes in the school, only the simulation test is carried out in the first part of this Section.

In the test of single bump condition, let the vehicle pass the bump at 15 km/h、25 km/h and 35 km/h respectively. In the test of two bump condition, the speed 35 km/h is dropped. The responses at different positions are collected by using the data acquisition equipment.

The preview control effect under the condition of single bump is shown in Figure 10(a), (b), (c)and Table 7.

The preview control effect under the condition of two bumps whose distance between each other is 43.5m is shown in Figure 11(a), (b), (c)and Table 7.

Compared between the speed of 25 km/h and 15 km/h, the greater the speed, the more obvious the performance improvement caused by predictive control.

When passing two bumps continuously, the power spectral density of suspension vibration with and without predictive control is mostly in low-frequency at low speed.

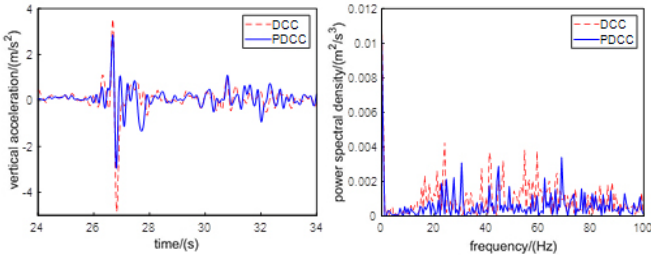

vertical acceleration power spectral density

(a) Simulation test results of passing a bump at a constant speed (15km / h)

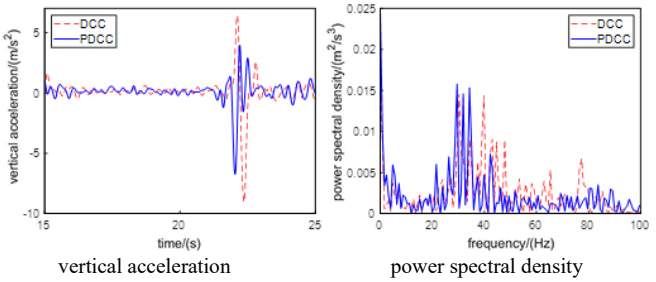

vertical acceleration power spectral density

(b) Simulation test results of passing a single bump at a constant speed (25km / h)

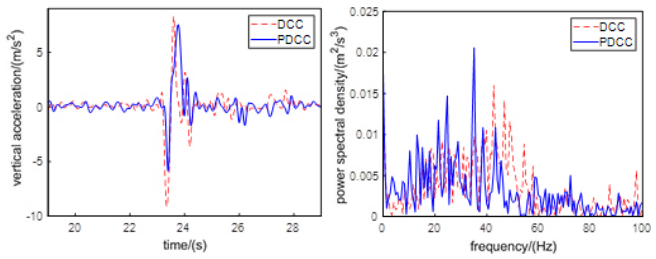

(c) Simulation test results of passing a single bump at a constant speed (35km / h)

Figure 10. Comparison of test results at different speeds

Table 7. Real vehicle test results under single or two bumps

Indices/Variables / Condition	Speed (km/h)	VDV Without Preview (m/s1.75)	VDV With Preview (m/s1.75)	Improvement
Single bump	15	1.4242	1.3148	7.68%
	25	2.6729	1.6260	39.17%
	35	3.2694	2.3094	29.36%
Two bumps	15	1.9554	1.5750	19.45%
	25	3.1307	2.1455	31.46%

8. CONCLUSIONS

This paper presents a preview dynamic chassis control strategy based on machine vision. The machine vision method is introduced on the basis of the fuzzy logic control strategy. The control current of shock absorber when the vehicle passes the bump is calculated before the vehicle has passed the bump, so that the shock absorber response is in advance. In this paper, YOLO is used to identify the bump and pothole. The monocular vision based model for calculating the distance of bump and pothole is introduced into this paper. The effectiveness of the strategy is verified by simulation and real vehicle test. Compared with the fuzzy logic control strategy, the acceleration response of the vehicle body under the preview control strategy has been reduced to different degrees at different speeds. At present, the best control current is obtained by experiment, which is lack of generality. Based on above excuse, the optimal control current calculation model based on the physical model of bump or pothole and quarter vehicle model of semi-active suspension will be studied in the future work.

REFERENCES

Ren Yongsheng, Zhou Jianpeng. (2006). Review of automotive semi active suspension technology. *Vibration and shock*, 25 (003): 162-165.

Chen long, Ma Rui, Wang Shoujing, Huang Chen, sun Xiaoqiang, Cui Xiaoli. (2020). Research on damping multi-mode switching control of vehicle semi-active suspension. *Vibration and impact*, 39 (13): 148-155.

Tianjun Z, Wan H, Wang Z, et al. Model reference adaptive control of semi-active suspension model based on AdaBoost algorithm for rollover prediction[J]. SAE International Journal of Vehicle Dynamics, Stability, and NVH, 2021, 6(10-06-01-0005).

Shehata Gad A. Preview model predictive control controller for magnetorheological damper of semi-active suspension to improve both ride and handling[J]. SAE International Journal of Vehicle Dynamics, Stability, and NVH, 2020, 4(10-04-03-0021).

Ye Guanghu, Wu Guangqiang. (2015). Simulation of semi active air suspension with magnetorheological damper. *Automotive engineering*, 37 (5): 560-565.

Deng Ming, Hua Yanqiu, Wu Guangqiang. Simulation and experimental validation of damping characteristic for a valve-controlled adjustable shock absorber[J]. International Journal of Vehicle Performance, 2018, 4(2): 133-154.

Zhang liangxiu, Wu Guangqiang, Wei Xinhui. (2020). Multi mode vertical control and real vehicle verification of vehicle dynamic chassis control system. *Science technology and engineering*, 20 (27): 11347-11352.

Zhang Xiangrui. (2020). Multi objective optimization control of vehicle semi-active suspension. Harbin Institute of technology.

Wu Guangqiang. Automotive Theory[M]. 3rd ed. Beijing: China Communications Press, 2021.

Redmon J, Divvala S, Girshick R, et al. (2015). You only look once: Unified, real-time object detection.

Wei Yongming, Quan Jicheng, Hou Yuqingyang. Research on UAV aerial image positioning based on YOLO V2. Progress in laser and optoelectronics, 054 (011): 95-104.

Redmon J, Farhadi A. (2018). YOLOv3: An incremental improvement. *arXiv* e-prints.

Qiao S, Pang S, Luo G, et al. (2020). Automatic detection of cardiac chambers using an attention-based YOLOv4 framework from four-chamber view of fetal echocardiography.

Lin M, Chen C, Lai C. (2019). Object detection algorithm based AdaBoost residual correction Fast R-CNN on network. The 2019 3rd International Conference.

Comer D E, Stevens D L. (1993). Internetworking with TCP/IP, Vol. III: Client-server programming and applications, Linux/Posix Sockets Version. Prentice Hall PTR.